

Complexation of 6-(4'-(toluidinyl)naphthalene-2-sulfonate by β -cyclodextrin and linked β -cyclodextrin dimers†

Duc-Truc Pham,^a Philip Clements,^a Christopher J. Easton,^b John Papageorgiou,^a Bruce L. May^a and Stephen F. Lincoln^{*a}

Received (in Montpellier, France) 16th October 2007, Accepted 18th December 2007

First published as an Advance Article on the web 21st January 2008

DOI: 10.1039/b715985d

The complexation of 6-(4'-(toluidinyl)naphthalene-2-sulfonate, TNS[−], by β -cyclodextrin (β CD) and five linked β CD-dimers is characterized by UV-Vis, fluorescence and ¹H NMR spectroscopy. In aqueous phosphate buffer at pH 7.0, *I* = 0.10 mol dm^{−3} and 298.2 K, TNS[−] forms host–guest complexes with β CD of stoichiometry β CD·TNS[−] {*K*₁ = [β CD·TNS[−]]/([β CD][TNS[−]]) = 3300 dm³ mol^{−1}} and β CD₂·TNS[−] {*K*₂ = [β CD₂·TNS[−]]/([β CD][β CD·TNS[−]]) = 11 dm³ mol^{−1}} as shown by fluorescence studies. For *N,N*-bis((2^A-dextrin)-S,3^AS)-3^A-deoxy-3^A- β -cyclodextrin)succinamide, 33 β CD₂su, *N*-((2^AS,3^AS)-3^A-deoxy-3^A- β -cyclodextrin)-*N'*-(6^A-deoxy-6^A- β -cyclodextrin)urea, 36 β CD₂su, *N,N*-bis(6^A-deoxy-6^A- β -cyclodextrin)succinamide, 66 β CD₂su, *N*-((2^AS,3^AS)-3^A-deoxy-3^A- β -cyclodextrin)-*N'*-(6^A-deoxy-6^A- β -cyclodextrin)urea, 36 β CD₂ur, and *N,N*-bis(6^A-deoxy-6^A- β -cyclodextrin)urea, 66 β CD₂ur, the analogous *K*₁ = 9600, 8700, 12 500, 9800, and 38 000 dm³ mol^{−1}, respectively. ¹H NMR ROESY studies provide evidence for variation of the mode of complexation of the TNS[−] guest as the host is changed. The factors affecting complexation are discussed and the synthesis of the new linked β CD-dimer 36 β CD₂su is reported.

Introduction

Studies of host–guest complexation by cyclodextrin (CD) hosts and their modified forms is an area of significant supramolecular chemical interest.¹ Prominent in such studies are linked CD-dimers^{2–4} in which the linker may be substituted onto the CD at either the C2^A, C3^A or C6^A carbon of a glucopyranose unit.^{5–7} This and the nature of the linker can significantly influence ditopic guest complexation and aspects of this are explored here.^{8–14}

This study is based on β -cyclodextrin, β CD, the α -1,4-linked heptamer of glucopyranose where the 7 primary and 14 secondary hydroxy groups delineate the narrow and wide ends of an annulus whose hydrophobic interior is lined with methine and methylene hydrogens and ether oxygens, and five linked β CD-dimers in which the linker is substituted either at C3^A (with inversion at C2^A and C3^A) or at C6^A of β CD as shown in Fig. 1 (where A signifies the substituted glucopyranose unit with neighboring units designated sequentially from B to G in a clockwise direction when viewed from the primary hydroxy group β CD end). These dimers are *N,N*-bis((2^AS,3^AS)-3^A-deoxy-3^A- β -cyclodextrin)succinamide, 33 β CD₂su, *N*-((2^AS,3^AS)-3^A-deoxy-3^A- β -cyclodextrin)-*N'*-(6^A-deoxy-6^A- β -cyclodextrin)urea, 36 β CD₂su,

N,N-bis(6^A-deoxy-6^A- β -cyclodextrin)succinamide, 66 β CD₂su, *N*-((2^AS,3^AS)-3^A-deoxy-3^A- β -cyclodextrin)-*N'*-(6^A-deoxy-6^A-

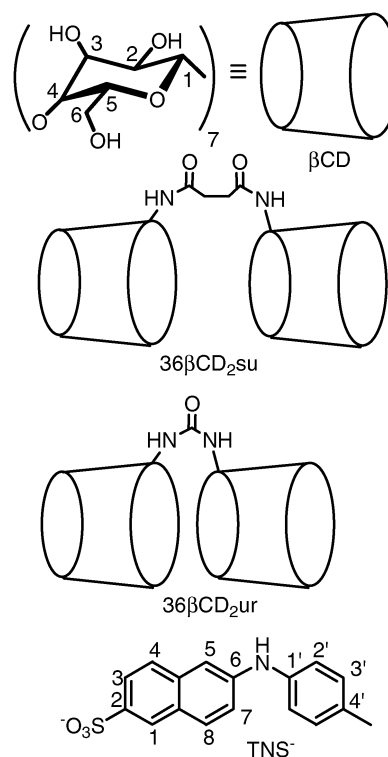


Fig. 1 Structures of β CD species and TNS[−]. In 33 β CD₂su both β CD are linked through C3^A, and in 66 β CD₂su and 66 β CD₂ur both β CD are linked through C6^A.

^a School of Chemistry and Physics, University of Adelaide, South Australia, 5005, Australia. E-mail: stephen.lincoln@adelaide.edu.au

^b Research School of Chemistry, Australian National University, Canberra, ACT 0200, Australia

† Electronic supplementary information (ESI) available: Additional UV-Vis, fluorescence and 1D ¹H and ¹³C NMR and 2D ¹H ROESY NMR spectra, associated data fits and molecular models are shown in Fig. S1–S34. See DOI: 10.1039/b715985d

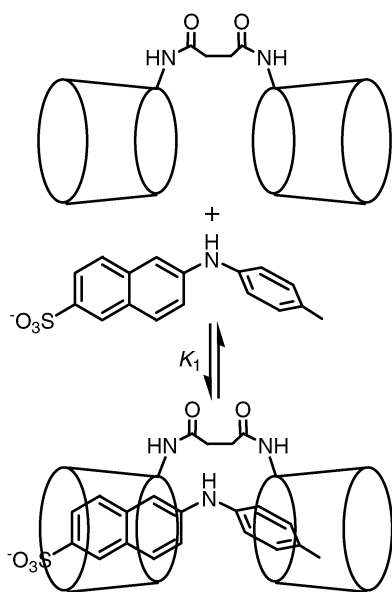


Fig. 2 Complexation equilibrium for 66βCD₂su and TNS[−].

β-cyclodextrin)urea, 36βCD₂ur, and *N,N*-bis(6^A-deoxy-6^A-β-cyclodextrin)urea, 66βCD₂ur. The aim is to find how the linking of βCD in dimers and the inversion of the C2^A and C3^A carbons of the C3^A substituted βCD glucopyranose units of 33βCD₂su, 36βCD₂su, and 36βCD₂ur affect complex stability.

The short succinamide and urea linkers were chosen to minimize the distance between the hydrophobic interiors of the βCD annuli with the expectation that this would approximately match the separation of hydrophobic aromatic components of the guest 6-(4'-(toluidinyl)-naphthalene-2-sulfonate, TNS[−], and enhance its complexation (Fig. 2). This guest is chosen because its UV-Vis absorption and fluorescence are modified by βCD complexation and facilitate studies of host–guest complexation. Additionally, the ¹H NMR resonance frequencies of TNS[−] are sufficiently different from those of βCD for ROESY cross-peaks arising in the host–guest complexes to provide structural insight. Earlier complexation⁸ and spectroscopic¹⁵ studies of TNS[−] are discussed in conjunction with the new data.

Results and discussion

UV-Vis spectrophotometric studies

The variation of the TNS[−] spectrum with [βCD]_{total} is shown in Fig. 3. An algorithm for the formation of βCD·TNS[−], λ_{max}(H₂O)/nm 261 (ε/dm³ mol^{−1} cm^{−1} 21 700) and 315 (16 500) and βCD₂·TNS[−] λ_{max}(H₂O)/nm 259 (ε/dm³ mol^{−1} cm^{−1} 21 700) and 314 nm (16 500) which have very similar spectra, best fits these data and yields the bracketed spectral data. The derived *K*₁ (= [βCD·TNS[−]]/([βCD][TNS[−]]) and *K*₂ (= [βCD₂·TNS[−]]/([βCD][βCD·TNS[−]]) appear in Table 1. (All UV-Vis and fluorescence studies in this study were carried out in aqueous phosphate buffer at pH 7.0, *I* = 0.10 mol dm^{−3} and 298.2 K).

The variations of the TNS[−] UV-Vis spectrum in the presence of the five linked βCD-dimers are characterized by isosbestic points and are best-fitted by an algorithm for the

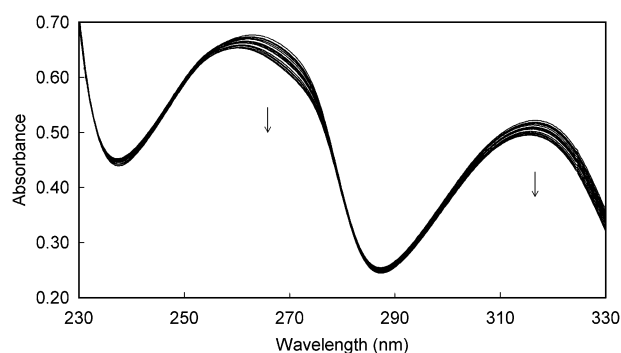


Fig. 3 UV-Vis absorption changes shown by TNS[−] (3.00×10^{-5} mol dm^{−3}) with [βCD]_{total} in the range 0, 3.03, 4.02, 4.97, 5.94, 6.93 and 8.87×10^{-5} , 1.12, 1.24, 1.37, 1.58, 1.80, 2.09, 2.39, 2.79, 3.17, 3.95, 4.46 and 4.96×10^{-4} mol dm^{−3}. The arrows indicate the direction of absorbance change as [βCD]_{total} increases.

formation of dominant binary complexes exemplified by 66βCD₂su·TNS[−]. The derived *K*₁ appear in Table 1. While the greatest change is induced in the spectrum of TNS[−] by 66βCD₂ur shown in Fig. 4 {λ_{max}(H₂O)/nm 276 (ε/dm³ mol^{−1} cm^{−1} 20 200) and 320 (20 700)} this difference is less for 36βCD₂ur (λ_{max} = 265 and 318 nm with ε = 20 600 and 17 300 dm³ mol^{−1} cm^{−1}, respectively). A similar relationship holds for 66βCD₂su {λ_{max}(H₂O)/nm 268 (ε/dm³ mol^{−1} cm^{−1} 19 200) 319 (18 000)} and 36βCD₂su {λ_{max}(H₂O)/nm 262 (ε/dm³ mol^{−1} cm^{−1} 19 900) and 317 (17 000)} and 33βCD₂su {λ_{max}(H₂O)/nm 264 (ε/dm³ mol^{−1} cm^{−1} 21 000) and 317 nm (16 900)}. These variations reflect changes in TNS[−] hydration in the complexed environment and possibly minor changes in the angles between the planes of the naphthyl and phenyl groups of TNS[−] to optimize complexation in the linked βCD-dimers. (Modeling of TNS[−] in the gas phase through the MM2 Chem3D protocol¹⁶ shows the naphthyl C6-NH-phenyl C1' angle to be 122° and the planes of the naphthyl and phenyl groups to be rotated 60° with respect to each other.)

The C3^A and C6^A substituted βCD of 33βCD₂su and 66βCD₂su and 66βCD₂ur, respectively, limit TNS[−] simultaneously complexed in both annuli to a single orientation with respect to the primary and secondary hydroxy ends of the βCD annuli (Fig. 1), while complexation in 36βCD₂su and

Table 1 Complexation constants, *K*₁ and *K*₂, determined by UV-Vis and fluorescence spectroscopy in aqueous phosphate buffer at pH 7.0, *I* = 0.10 mol dm^{−3} and 298.2 K

Host	UV-Vis 10 ^{−3} × <i>K</i> ₁ ^a dm ³ mol ^{−1}	Fluorescence 10 ^{−3} × <i>K</i> ₁ ^a dm ³ mol ^{−1}
βCD	3.02 ± 0.03	3.30 ± 0.01 (3.14) ^b
33βCD ₂ su	10.7 ± 0.5	9.60 ± 0.05
36βCD ₂ su	10.9 ± 0.2	8.7 ± 0.02
66βCD ₂ su	16.1 ± 0.1	12.5 ± 0.1 (16.7) ^b
36βCD ₂ ur	18.3 ± 0.4	9.80 ± 0.02
66βCD ₂ ur	55.1 ± 0.3	38.0 ± 0.1 (45.2) ^b
	<i>K</i> ₂ ^a dm ³ mol ^{−1}	<i>K</i> ₂ ^a dm ³ mol ^{−1}
βCD	57.2 ± 0.6	11.0 ± 0.6 (86) ^b

^a The errors shown are those obtained from data fitting. When experimental error is taken into account the overall error is ±3%. ^b Data from ref. 8. The fluorimetric signal to noise ratio is superior in the present study.

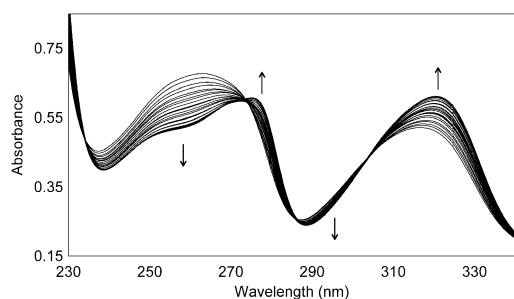


Fig. 4 UV-Vis absorption changes shown by TNS^- ($3.00 \times 10^{-5} \text{ mol dm}^{-3}$) with $[\text{66}\beta\text{CD}_2\text{ur}]_{\text{total}}$ in the range 0, 4.04 , and 8.20×10^{-6} , and 1.21 , 1.61 , 1.99 , 2.39 , 2.64 , 3.16 , 3.57 , 3.94 , 4.50 , 4.98 , 5.50 , 6.33 , 7.18 , 8.34 , and 9.51×10^{-5} , and 1.11 , 1.26 , 1.42 , 1.58 , 1.77 , and $1.96 \times 10^{-4} \text{ mol dm}^{-3}$. The arrows indicate the direction of absorbance change as $[\text{66}\beta\text{CD}_2\text{ur}]_{\text{total}}$ increases. Isosbestic points occur at 234.5 , 273.5 , 286 and 304 nm .

$36\beta\text{CD}_2\text{ur}$ offers two possible isomeric pairs of TNS^- complexes in each case.

Fluorimetric studies

The relative fluorescence increases shown by TNS^- on complexation by βCD are best-fitted by an algorithm for the formation of $\beta\text{CD}\cdot\text{TNS}^-$ and $\beta\text{CD}_2\cdot\text{TNS}^-$ characterized by K_1 and K_2 , respectively (Table 1). The greater fluorescence changes induced by the linked βCD -dimers, exemplified by those of $66\beta\text{CD}_2\text{ur}\cdot\text{TNS}^-$ (Fig. 5), are best fitted by an algorithm for the dominant formation of a linked βCD -dimer $\cdot\text{TNS}^-$ complex. The derived K_1 appear in Table 1. Time resolved studies show the fluorescence lifetime of TNS^- in water to be 60 ps and $\sim 2500 \text{ ps}$ when complexed by βCD such that the K_1 and K_2 derived through fluorescence spectroscopy refer to ground state equilibria and should be similar to those derived through UV-visible studies.¹⁷ Generally this is the case (Table 1) and where differences occur it is probable that the values derived through fluorescence measurements are more reliable because of the greater spectral changes observed in these studies.

In the free state, the TNS^- fluorescence maxima, λ_{max} , occur at 408 and 488 nm with relative fluorescences of 2.0 a.u.

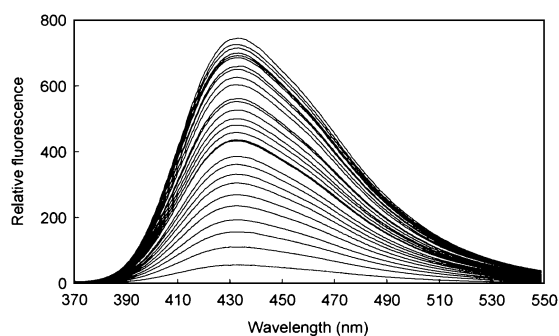


Fig. 5 Increase in the relative fluorescence of TNS^- ($1.00 \times 10^{-6} \text{ mol dm}^{-3}$) with $[\text{66}\beta\text{CD}_2\text{ur}]_{\text{total}}$ in the range 0, 1.96 , 3.96 , 5.92 and 7.92×10^{-6} and 1.00 , 1.24 , 1.48 , 1.73 , 2.00 , 2.32 , 2.61 , 2.94 , 3.26 , 3.63 , 3.95 , 4.47 , 4.94 , 5.49 , 6.32 , 7.20 , 8.42 and 9.57×10^{-5} , and 1.08 , 1.20 , 1.32 , 1.44 , 1.60 , 1.80 and $1.99 \times 10^{-4} \text{ mol dm}^{-3}$. The excitation wavelength is 320 nm .

(arbitrary units) and 0.5 a.u. , respectively. The fluorescence of $\beta\text{CD}\cdot\text{TNS}^-$ (473 nm , 9 a.u.) is consistent with complexation changing the TNS^- environment and enhancing fluorescence as a consequence of partial complexation in the βCD annulus. Greater decreases in λ_{max} and increases in relative fluorescence occurs for $\beta\text{CD}_2\cdot\text{TNS}^-$ (435 nm , 104 a.u.), $66\beta\text{CD}_2\text{su}\cdot\text{TNS}^-$ (437 nm , 327 a.u.), $36\beta\text{CD}_2\text{su}\cdot\text{TNS}^-$ (438 nm , 230 a.u.), $33\beta\text{CD}_2\text{su}\cdot\text{TNS}^-$ (439 nm , 245 a.u.), $66\beta\text{CD}_2\text{ur}\cdot\text{TNS}^-$ (433 nm , 790 a.u.), and $36\beta\text{CD}_2\text{ur}\cdot\text{TNS}^-$ (442 nm , 350 a.u.) as a result of TNS^- experiencing an increased environment change when complexed in two βCD annuli.

The decrease in λ_{max} is consistent with the existence of three excited states of TNS^- whose relative populations are dependent on environment.¹⁵ Excitation ($\pi \rightarrow \pi^*$) from the $\text{TNS}^- S_0$ ground state in which the planes of the naphthyl and phenyl groups are rotated 60° with respect to each other results in three TNS^- excited states. Using the reported nomenclature, the first is $S_{1,\text{np}}$ (excitation $\lambda_{\text{max}} = 320 \text{ nm}$, emission $\lambda_{\text{max}} = 460 \text{ nm}$) in which the rotation is retained. Electron transfer produces two TNS^- charge transfer excited states: $S_{1-\text{ct},\text{np}}$ (excitation $\lambda_{\text{max}} = 320\text{--}330 \text{ nm}$, emission $\lambda_{\text{max}} \sim 495 \text{ nm}$) in which the naphthyl and phenyl planes approach coplanarity, and $S_{1-\text{ct},\text{perp}}$ (excitation $\lambda_{\text{max}} = 290 \text{ nm}$, emission $\lambda_{\text{max}} = 400 \text{ nm}$) in which the naphthyl and phenyl planes are thought to be perpendicular to each other. In water the $S_{1-\text{ct},\text{perp}}$ excited state dominates as a result of water hydrogen bonding to the amine nitrogen of TNS^- while $S_{1-\text{ct},\text{np}}$ is much less populated and $S_{1,\text{np}}$ is even less populated (Fig. 6).

However, in non-polar and viscous solvents $S_{1,\text{np}}$ becomes dominantly populated. The latter solvent conditions resemble the hydrophobic and motion restricting environment which TNS^- experiences in the βCD annulus. Accordingly, the decrease of the observed emission λ_{max} for TNS^- in the linked βCD -dimer complexes is consistent with $S_{1,\text{np}}$ becoming the dominant excited state, as shown for $66\beta\text{CD}_2\text{ur}\cdot\text{TNS}^-$ in Fig. 7, whereas the observed $\lambda_{\text{max}} = 408 \text{ nm}$ for TNS^- in water (Fig. 6) is a consequence of emission from the dominant

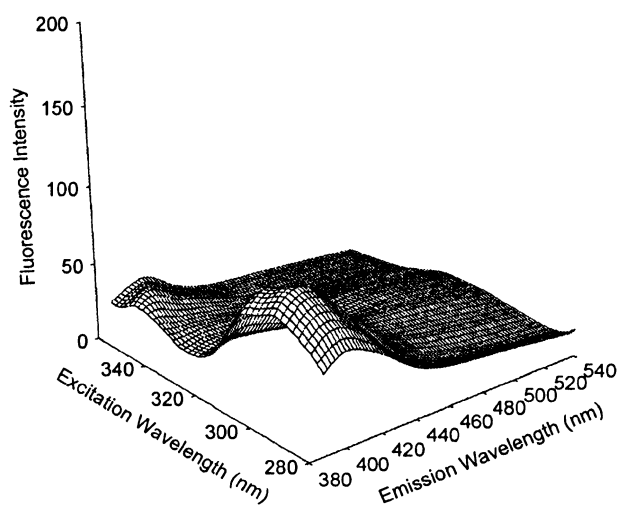


Fig. 6 Three dimensional plot of the fluorescence of TNS^- ($1.0 \times 10^{-5} \text{ mol dm}^{-3}$) as a function of excitation and emission wavelength at 2 nm intervals.

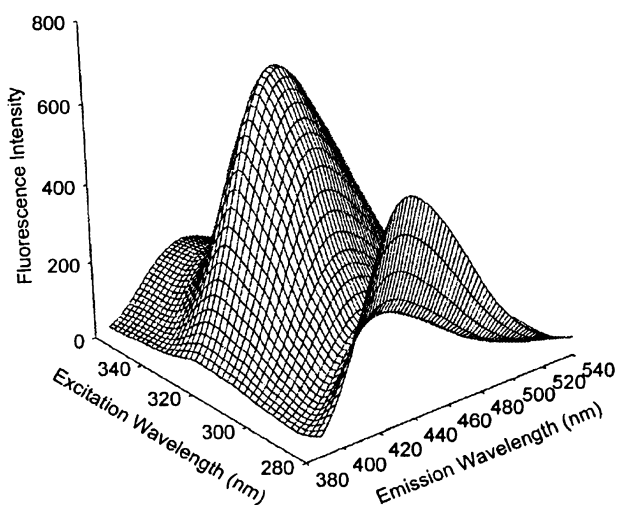


Fig. 7 Three dimensional plot of the fluorescence of TNS^- ($1.0 \times 10^{-6} \text{ mol dm}^{-3}$) and $66\beta\text{CD}_2\text{ur}$ ($1.0 \times 10^{-5} \text{ mol dm}^{-3}$) as a function of excitation and emission wavelength at 2 nm intervals. Under these conditions $[\beta\text{CD}_2\text{ur} \cdot \text{TNS}^-] = 0.27 \times 10^{-6} \text{ mol dm}^{-3}$.

$S_{1-\text{ct,perp}}$ excited state. In Fig. 7, the much greater fluorescence of $66\beta\text{CD}_2\text{ur} \cdot \text{TNS}^-$ dominates that of TNS^- .

The increased TNS^- fluorescence with complexation probably results from a combination of three factors. The first is the decrease in the relative populations of the charge transfer $S_{1-\text{ct,np}}$ and $S_{1-\text{ct,perp}}$ excited states, which are likely to decay more rapidly than the $S_{1,\text{np}}$ excited state. The second is the isolation of TNS^- from the quenching pathway provided by water oscillators, and the third is the decrease in the number of rotational degrees of freedom for TNS^- which is likely to decrease the effectiveness of quenching.¹⁸

2D ^1H ROESY NMR studies

The 2D ^1H ROESY NMR spectra of D_2O solutions $1.50 \times 10^{-3} \text{ mol dm}^{-3}$ in TNS^- and 1.50×10^{-3} and $3.00 \times 10^{-3} \text{ mol dm}^{-3}$ in βCD (Fig. 8) are similar with weak cross-peaks arising from methyl proton interaction with βCD H5 and stronger cross-peaks arising from naphthyl and phenyl dipolar interactions with H3 and H5 within the βCD annulus. (All ^1H NMR studies were carried out in phosphate buffer solution at pD 7.0, $I = 0.10 \text{ mol dm}^{-3}$, and 298.2 K.) On this basis it is assumed that the remaining upfield cross-peaks arise from dipolar interactions with H6, although the H6 resonance is not clearly distinguishable from H2 and H4.¹⁹ This indicates the formation of at least two of the four possible $\beta\text{CD} \cdot \text{TNS}^-$ isomers in which βCD has either its primary or secondary hydroxy face adjacent to the amine group of TNS^- . Four isomers arising from the pairing of any two of these βCD orientations are possible for $\beta\text{CD}_2 \cdot \text{TNS}^-$ but their precise identification is unclear from these data.

The 2D ^1H ROESY NMR spectrum of a D_2O solution $1.50 \times 10^{-3} \text{ mol dm}^{-3}$ in TNS^- and $66\beta\text{CD}_2\text{su} \cdot \text{TNS}^-$ (Fig. 9) shows strong cross-peaks between all TNS^- protons and those of $66\beta\text{CD}_2\text{su}$ whose spectrum shows many more resonances by comparison with βCD as a consequence of the inequivalence of the seven glucopyranose units. Strong cross-peaks are shown by $66\beta\text{CD}_2\text{ur} \cdot \text{TNS}^-$ and weaker cross-peaks are shown

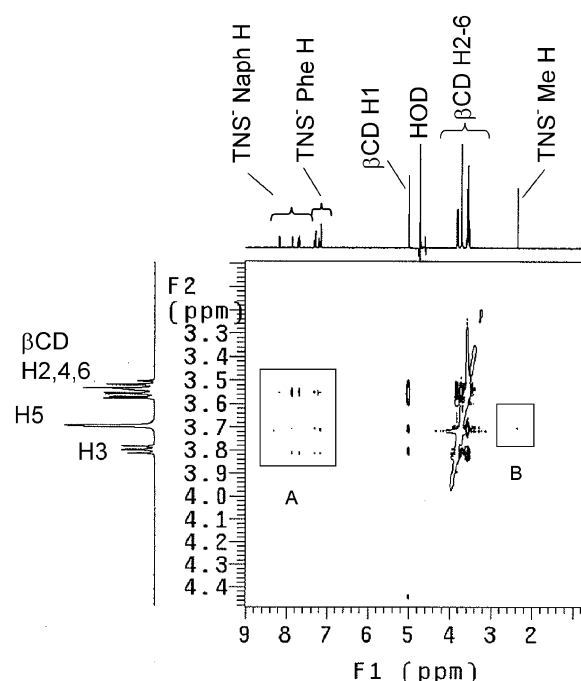


Fig. 8 2D ^1H ROESY NMR (600 MHz) spectrum of a D_2O solution equimolar at $1.50 \times 10^{-3} \text{ mol dm}^{-3}$ in TNS^- and βCD . The rectangles A and B contain the cross-peaks arising from the NOE interactions between the annular H3, H5 and H6 protons of βCD and the aromatic and methyl protons of TNS^- , respectively.

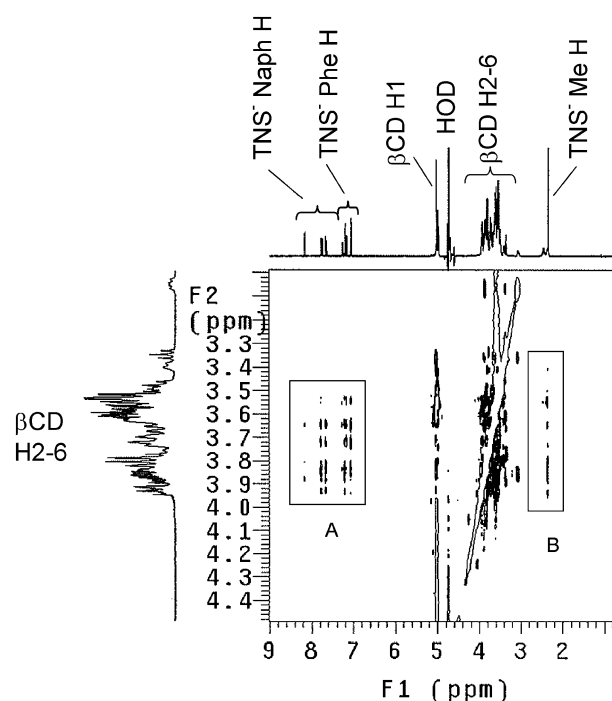


Fig. 9 2D ^1H ROESY NMR (600 MHz) spectrum of a D_2O solution equimolar at $1.50 \times 10^{-3} \text{ mol dm}^{-3}$ in TNS^- and $66\beta\text{CD}_2\text{su}$. The rectangles A and B contain the cross-peaks arising from the NOE interactions between the annular H3, H5 and H6 protons of $66\beta\text{CD}_2\text{su}$ and the aromatic and methyl protons of TNS^- , respectively.

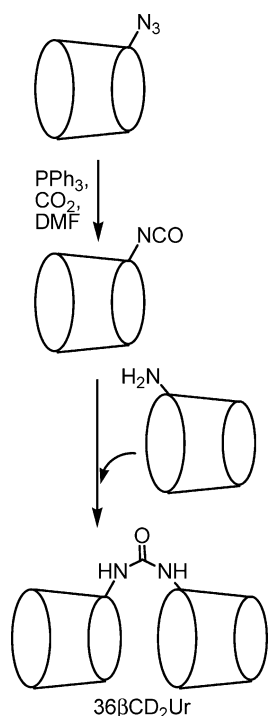


Fig. 10 Synthesis of 36βCD₂ur.

by 36βCD₂su·TNS[−] and 33βCD₂su·TNS[−]. The spectrum of 36βCD₂ur·TNS[−] shows a very weak cross-peak for the methyl group of TNS[−] which may indicate that this group is distant from 36βCD₂ur protons.

The chemical shifts of the TNS[−] resonances with concentration over a 20-fold variation show no systematic change consistent with little self-association occurring.

Synthesis

The 33βCD₂su, 36βCD₂su, 66βCD₂su, and 66βCD₂ur linked βCD dimers were prepared as previously described.⁷ The new 36βCD₂ur was prepared in 66% yield by reacting (2^AS,3^AS)-amino-3^A-deoxy-3^A-β-cyclodextrin in CO₂ saturated DMF in the presence of triphenyl-phosphine (Fig. 10). However, attempts to prepare the 33βCD₂ur dimer by linking two (2^AS,3^AS)-3^A-deoxy-3^A-azido-β-cyclodextrins through reaction with CO₂ failed as did attempts to link two (2^AS,3^AS)-3^A-deoxy-3^A-amino-β-cyclodextrins through reaction with diphenyl carbonate, probably because the C3^A inversions in both C3^A substituted βCDs cause too much steric crowding for reaction to occur. This is consistent with the combination of the C3^A inversion and the shortness of the urea linker preventing the formation of 33βCD₂ur. Coincidentally, the secondary hydroxy end to secondary hydroxy end dimer, corresponding to the 33βCD₂su and putative 33βCD₂ur dimer, is the energetically most favored dimerization for αCD, βCD and γCD monomers in the gas phase (and also in aqueous solution for αCD).²⁰

Molecular modeling

The succinamide linker is more flexible than the urea linker, and joining the linker to βCD through a primary C6^A carbon appears to allow more flexibility than joining through a

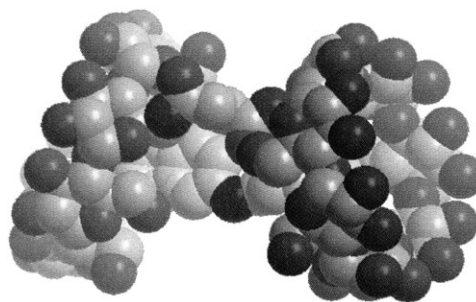


Fig. 11 The energy minimized 66βCDsu·TNS[−] model. The naphthalene ring adjacent to the guest nitrogen appears between the succinamide-linked βCDs. Hydrogen atoms are omitted.

secondary inverted C3^A carbon. In MM2 Chem3D¹⁶ energy minimized gas phase models of the linked βCD-dimers, in which the βCD annuli are constrained to an approximately common axis by the TNS[−] guest, the distance from O3^B to O6^B in the glucopyranose unit of βCD is 780 pm. The distances measured from the mid-point of this distance projected into the centre of each of the linked βCD annuli are 1240 pm (~0°) for 33βCD₂su, 1350 pm (~0°) for 36βCD₂su and 1410 pm (~30°) for 66βCD₂su (Fig. 11), where the values in brackets are the angles between the planes of the two βCD macrocycles. Because of the shortness of the urea linker and the constraining effect of the inverted C3^A carbon joined to the linker, the planes of the βCD annuli in 36βCD₂ur are arranged at ~60° to each other such that the centers of the annuli are separated by 1120 pm. The corresponding distance in 66βCD₂ur is 980 pm (~40°) seemingly as a result of the greater flexibility afforded to both ends of the linker joining the two βCD through primary C6^A carbons. These distances compare with 1040 pm from the naphthyl C2 to the phenyl C4' of TNS[−] (Fig. 1) and give an indication of the change in interannular distances caused by the different linking βCD carbon atoms in the gas phase.

While hydrogen bonding between the βCD hydroxy groups and water occurs, the structural constraints discussed above probably maintain the relative sizes of the interannular distances. The interannular distance is not the only arbiter of complex stability. This is shown by 66βCD₂ur and 36βCD₂ur with the shortest and second shortest distances, respectively, forming the most and second most stable complexes with TNS[−] while 66βCD₂su with the longest distance forming the third most stable complex (Table 1). Evidently, the angles between the planes of the βCD annuli and the presence of a C3^A inversion also influence relative complex stabilities.

Conclusion

Generally, the *K*₁ and *K*₂ determined from UV-Vis absorbance changes are either similar to or greater than those determined from fluorescence changes (Table 1). Because the UV-Vis changes are less than the fluorescence changes it is probable that the *K*₁ and *K*₂ determined from the latter changes are the more reliable. The magnitude variation of both sets of formation constants for the linked βCD-dimer TNS[−] complexes show similar trends where the *K*₁ determined from UV-Vis

measurement range from 3.5 to 18.2 times greater than K_1 for $\beta\text{CD}\cdot\text{TNS}^-$ and those determined from fluorescence measurements are 2 to 11.5 times greater than K_1 for $\beta\text{CD}\cdot\text{TNS}^-$ as seen from Table 1. The K_1 variations for the linked βCD -dimer complexes are consistent with $\text{C6}^{\text{A}}\text{--}\text{C6}^{\text{A}}$ linking of βCD and shortening of the linker maximizing stability. The C2^{A} and C3^{A} inversions in the $\text{C3}^{\text{A}}\text{--}\text{C6}^{\text{A}}$ and $\text{C3}^{\text{A}}\text{--}\text{C3}^{\text{A}}$ linked βCD annuli decrease their ability to complex TNS^- . The K_2 for the stepwise formation of $\beta\text{CD}_2\cdot\text{TNS}^-$ is much less than K_1 for $\beta\text{CD}\cdot\text{TNS}^-$ than anticipated statistically. This suggests that complexation of a second βCD by TNS^- is hindered by the presence of βCD in $\beta\text{CD}\cdot\text{TNS}^-$.

The formation of binary βCD host–guest complexes in water with a wide range of guests exemplified by benzoate,²¹ benzoic acid,²¹ *p*-dimethylaminoazobenzenesulfonate (Methyl Orange anion),²² deoxycholate,¹³ adamantane-1-carboxylate,¹⁰ 6-(*p*-(*tert*-butyl)-phenyl) naphthalene-2-sulfonate (BNS^-)¹⁰ is characterized by a wide stability range as shown by their $K_1 = 60, 590, 2160, 4844, 39\,500$, and $55\,700\text{ dm}^3\text{ mol}^{-1}$, respectively. The mid-range position of TNS^- in this series ($K_1 = 3020\text{ dm}^3\text{ mol}^{-1}$) contrasts with the 13-fold stronger βCD complexation of BNS^- which is identical to TNS^- except that a methyl group is replaced by a *tert*-butyl group in BNS^- . The effect of this change illustrates the subtlety of the combination of effects affecting relative host–guest complex stabilities.

Experimental section

Instrumental

UV-Vis spectra were recorded at 0.25 nm intervals using a Cary 5000 UV-Vis spectrophotometer in matched 1 cm quartz cells. Spectra were run against reference solutions containing identical concentrations of either βCD or a linked βCD -dimer as that in the TNS^- solutions. Fluorescence spectra were recorded at 0.5 nm intervals using a Cary Eclipse fluorimeter with excitation and emission slit widths of 5 and 10 nm, respectively. Samples were thermostated at $298.2 \pm 0.02\text{ K}$. Solutions were prepared in phosphate buffer at pH 7.0 and $I = 0.10\text{ mol dm}^{-3}$ in both studies. For characterization of $36\beta\text{CD}_2\text{ur}$ ^1H and ^{13}C 1D NMR spectra of D_2O solutions buffered at pD 7.0 (phosphate buffer, $I = 0.10\text{ mol dm}^{-3}$, 298.2 K) were run in 5 mm NMR tubes thermostated at $298.2 \pm 0.1\text{ K}$ on a Varian Gemini ACP-300 MHz NMR spectrometer operating at 300.145 and 75.4 MHz, respectively. The ^1H 2D ROESY NMR spectra for the six host–guest systems studied were run on a Varian Inova 600 NMR spectrometer operating at 599.957 MHz with a delay time of 300 ms. Chemical shifts were measured from external trimethylsilylpropionic acid in D_2O .

Materials

Potassium-6-(4'-(toluidinyl)naphthalene-2-sulfonate (Sigma), KTNS, was twice recrystallized from water and vacuum dried to constant weight prior to use. Phosphate buffer was prepared from Na_2HPO_4 (BDH) and KH_2PO_4 (Ajax) according to literature procedures.²³ β -Cyclodextrin was a gift from Nihon Shokuhin Kako Co. and was used without further purification.

All other reagents were of good quality reagent grade. The linked βCD -dimers $33\beta\text{CD}_2\text{su}$, $36\beta\text{CD}_2\text{su}$, $66\beta\text{CD}_2\text{su}$, $36\beta\text{CD}_2\text{ur}$, and $66\beta\text{CD}_2\text{ur}$ were prepared as in the literature and melting points, elemental analyses and ^1H 1D NMR spectra in good agreement with those reported were obtained.⁷

Synthesis of *N*-((2^A*S*,3^A*S*)-3^A-deoxy-3^A- β -cyclodextrin)-*N'*-(6^A-deoxy-6^A- β -cyclodextrin)urea, $36\beta\text{CD}_2\text{ur}$. (2^A*S*,3^A*S*)-3^A-Amino-3^A-deoxy-3^A- β -cyclodextrin (1.24 g, 0.88 mmol) was dissolved in 10 dm^3 DMF and stirred at room temperature while dry CO_2 was bubbled through the solution. After 1 h, 6^A-deoxy-6^A-azido- β -cyclodextrin (918 mg, 0.79 mmol) in DMF (5 dm^3) was added dropwise followed by triphenylphosphine (288 mg, 1.11 mmol) in DMF (10 dm^3). The solution was stirred overnight after which TLC showed no 6^A-deoxy-6^A-azido- β -cyclodextrin remaining. After reduction in volume to 5 cm^3 , the reaction mixture was added to acetone. The precipitate was collected by vacuum filtration, washed with acetone and diethyl ether and dried under vacuum. The product was dissolved in H_2O and run through a BioRex 70 (H^+) column. Water was removed and the product was freeze dried to give a yield of 1.2 g (66%) (Found: C, 39.2; H, 6.5 N, 0.97. $\text{C}_{85}\text{H}_{140}\text{N}_2\text{O}_{69}\cdot 17\text{H}_2\text{O}$: requires C, 39.26; H, 6.74; N, 1.08%). LCQ-MS: ($\text{M} + \text{H}^+$) 2295.3; ($\text{M} + \text{Na}^+$) 2318.6. ^1H NMR: δ_{H} (300 MHz; D_2O ; $\text{Me}_3\text{Si}(\text{CH}_2)_3\text{SO}_3\text{H}$ external) 5.14–5.04 (m, 14H, H1); 3.9–3.4 (m, 84H, H2–H6). ^{13}C NMR: δ_{C} (74.4 MHz; D_2O ; $\text{Me}_3\text{Si}(\text{CH}_2)_3\text{SO}_3\text{H}$ external) 162.6 (amide C=O), 106.3–103.7 (C1), 85.5–82.4 (C4), 75.7–73.3 (C2, C3, C5), 62.9–62.3 (C6), 54.3 (C3^{A}), 43.2 (C6^{A}).

Data analysis

The appropriate algorithms were iteratively fitted to experimental data to determine K_1 and K_2 using an in-house program Specfit²⁴ for the UV-Vis and fluorescence data.

Acknowledgements

The award of a MOET scholarship by the Vietnamese Government to Duc-Truc Pham, and the support of this study by the Australian Research Council and the University of Adelaide and a gift of β -cyclodextrin from Nihon Shokuhin Kako Co., Japan, are gratefully acknowledged.

References

- (a) M. L. Bender and M. Komiyama, in *Cyclodextrin Chemistry*, Springer, Berlin, 1978; (b) J. Szejtli, *Chem. Rev.*, 1998, **98**, 1743; (c) G. Gattuso, S. A. Nepogodiev and J. F. Stoddart, *Chem. Rev.*, 1998, **98**, 1959; (d) C. J. Easton and S. F. Lincoln, in *Modified Cyclodextrins: Scaffolds and Templates for Supramolecular Chemistry*, Imperial College Press, London, 1999; (e) G. Wenz, B.-H. Han and A. Muller, *Chem. Rev.*, 2006, **106**, 782–817.
- A. Harada, *Acc. Chem. Res.*, 2001, **34**, 456–461.
- (a) J. S. Lock, B. L. May, P. Clements, S. F. Lincoln and C. J. Easton, *Org. Biomol. Chem.*, 2004, **2**, 1381–1386; (b) J. S. Lock, B. L. May, P. Clements, S. F. Lincoln and C. J. Easton, *J. Inclusion Phenom. Macrocyclic Chem.*, 2004, **50**, 13–18.
- Y. Liu and Y. Chen, *Acc. Chem. Res.*, 2006, **39**, 681–691.
- S.-H. Chiu, D. C. Myles, R. L. Garrell and J. F. Stoddart, *J. Org. Chem.*, 2000, **65**, 2792–2796.
- J. H. Coates, C. J. Easton, S. J. van Eyk, S. F. Lincoln, B. L. May, C. B. Walland and M. L. Williams, *J. Chem. Soc., Perkin Trans. 1*, 1990, 2619–2620.

- 7 C. J. Easton, S. J. van Eyk, S. F. Lincoln, B. L. May, J. Papageorgiou and M. L. Williams, *Aust. J. Chem.*, 1997, **50**, 9–14.
- 8 C. A. Haskard, C. J. Easton, B. L. May and S. F. Lincoln, *J. Phys. Chem.*, 1996, **100**, 14457–14461.
- 9 (a) C. A. Haskard, B. L. May, T. Kurucsev, S. F. Lincoln and C. J. Easton, *J. Chem. Soc., Faraday Trans.*, 1997, **93**, 279–282; (b) M. M. Cieslinski, P. Clements, B. L. May, C. J. Easton and S. F. Lincoln, *J. Chem. Soc., Perkin Trans. 2*, 2002, 947–952.
- 10 R. Breslow, N. Greenspoon, T. Guo and R. Zarzycki, *J. Am. Chem. Soc.*, 1989, **111**, 8296–8297.
- 11 (a) B. Zhang and R. Breslow, *J. Am. Chem. Soc.*, 1997, **119**, 1676–1681; (b) R. Breslow and S. D. Dong, *Chem. Rev.*, 1998, **98**, 1997–2011; (c) R. Breslow, S. Belvedere, L. Gershell and D. Leung, *Pure Appl. Chem.*, 2000, **72**, 333–342.
- 12 Y. Liu, B. Li, C.-C. You, T. Wada and Y. Inoue, *J. Org. Chem.*, 2001, **66**, 225–232.
- 13 Y. Liu, Y.-W. Yang, E.-C. Yang and X.-D. Guan, *J. Org. Chem.*, 2004, **69**, 6590–6602.
- 14 (a) L. C. West, O. Wyness, B. L. May, P. Clements, S. F. Lincoln and C. J. Easton, *Org. Biomol. Chem.*, 2003, **1**, 887–894; (b) O. Wyness, B. L. May, P. Clements, S. F. Lincoln and C. J. Easton, *Aust. J. Chem.*, 2004, **57**, 571–576.
- 15 K. K. Karukstis, D. A. Krekel, D. A. Weinberger, R. A. Bittker, N. R. Naito and S. H. Bloch, *J. Phys. Chem.*, 1995, **99**, 449–453.
- 16 Chem3D Ultra. CambridgeSoft Co., 100 Cambridge Park Drive, Cambridge, MA 02140 USA.
- 17 (a) A. Nakamura, K. Saitoh and F. Toda, *Chem. Phys. Lett.*, 1991, **187**, 110–115; (b) N. Sarkar, K. Das, D. Nath and K. Bhattacharyya, *Chem. Phys. Lett.*, 1992, **196**, 491–496; (c) N. Sarkar, K. Das, D. Nath and K. Bhattacharyya, *Chem. Phys. Lett.*, 1994, **218**, 492–498; (d) A. Datta, D. Mandal, S. K. Pal, S. Das and K. Bhattacharyya, *J. Chem. Soc., Faraday Trans.*, 1998, **94**, 3471–3475.
- 18 J. Hicks, M. Vandersall, Z. Babarogic and K. B. Eisenthal, *Chem. Phys. Lett.*, 1985, **116**, 18–24.
- 19 H.-J. Schneider, F. Hacket, V. Rüdiger and H. Ikeda, *Chem. Rev.*, 1998, **98**, 1755–17885.
- 20 (a) P. Bonnet, C. Jaime and L. Morin-Allory, *J. Org. Chem.*, 2001, **66**, 689–692; (b) C. S. Nascimento, C. P. A. Anconi, H. F. Dos Santos and W. B. De Almeida, *J. Phys. Chem. A*, 2005, **109**, 3209–3219.
- 21 S. E. Brown, J. H. Coates, P. A. Duckworth, S. F. Lincoln, C. J. Easton and B. L. May, *J. Chem. Soc., Faraday Trans.*, 1993, **87**, 1035–1040.
- 22 C. A. Haskard, B. L. May, T. Kurucsev, S. F. Lincoln and C. J. Easton, *J. Chem. Soc., Faraday Trans.*, 1997, **93**, 279–282.
- 23 E. J. King and W. M. Sperry, *Biochemists' Handbook*, Spon, London, 1971.
- 24 T. Kurucsev, University of Adelaide, 1984.